

REPORT DOCUMENTATION PAGE

Form Approved
OMB No. 0704-0188

Public reporting burden for this collection of information is estimated to average 1 hour per response, including the time for reviewing instructions, searching existing data sources, gathering and maintaining the data needed, and completing and reviewing this collection of information. Send comments regarding this burden estimate or any other aspect of this collection of information, including suggestions for reducing this burden to Department of Defense, Washington Headquarters Services, Directorate for Information Operations and Reports (0704-0188), 1215 Jefferson Davis Highway, Suite 1204, Arlington, VA 22202-4302. Respondents should be aware that notwithstanding any other provision of law, no person shall be subject to any penalty for failing to comply with a collection of information if it does not display a currently valid OMB control number. PLEASE DO NOT RETURN YOUR FORM TO THE ABOVE ADDRESS.

1. REPORT DATE (DD-MM-YYYY)

2. REPORT TYPE
Technical Papers

3. DATES COVERED (From - To)

4. TITLE AND SUBTITLE

5a. CONTRACT NUMBER

5b. GRANT NUMBER

5c. PROGRAM ELEMENT NUMBER

6. AUTHOR(S)

5d. PROJECT NUMBER

2303

5e. TASK NUMBER

m2c8

5f. WORK UNIT NUMBER

7. PERFORMING ORGANIZATION NAME(S) AND ADDRESS(ES)

Air Force Research Laboratory (AFMC)
AFRL/PRS
5 Pollux Drive
Edwards AFB CA 93524-7048

8. PERFORMING ORGANIZATION
REPORT

9. SPONSORING / MONITORING AGENCY NAME(S) AND ADDRESS(ES)

Air Force Research Laboratory (AFMC)
AFRL/PRS
5 Pollux Drive
Edwards AFB CA 93524-7048

10. SPONSOR/MONITOR'S
ACRONYM(S)

11. SPONSOR/MONITOR'S
NUMBER(S)

12. DISTRIBUTION / AVAILABILITY STATEMENT

Approved for public release; distribution unlimited.

13. SUPPLEMENTARY NOTES

14. ABSTRACT

15. SUBJECT TERMS

16. SECURITY CLASSIFICATION OF:

a. REPORT

Unclassified

b. ABSTRACT

Unclassified

c. THIS PAGE

Unclassified

17. LIMITATION
OF ABSTRACT

A

18. NUMBER
OF PAGES

19a. NAME OF RESPONSIBLE
PERSON

Leilani Richardson

19b. TELEPHONE NUMBER

(include area code)
(661) 275-5015

Standard Form 298 (Rev. 8-98)
Prescribed by ANSI Std. Z39.18

62 122024
separate items are enclosed

C8

MEMORANDUM FOR PRS (In-House Publication)

FROM: PROI (TI) (STINFO)

08 Dec 2000

SUBJECT: Authorization for Release of Technical Information, Control Number: **AFRL-PR-ED-TP-2000-234**
Schneider, Stefan (USC); Vij, A; Sheehy, J.A., et al. , "In Pursuit of the PO_2^+ Cation"

Journal – Z. Anorg. Allg. Chemie

(Statement A)

1. This request has been reviewed by the Foreign Disclosure Office for: a.) appropriateness of distribution statement, b.) military/national critical technology, c.) export controls or distribution restrictions, d.) appropriateness for release to a foreign nation, and e.) technical sensitivity and/or economic sensitivity.

Comments: _____

Signature _____ Date _____

2. This request has been reviewed by the Public Affairs Office for: a.) appropriateness for public release and/or b) possible higher headquarters review.

Comments: _____

Signature _____ Date _____

3. This request has been reviewed by the STINFO for: a.) changes if approved as amended, b) appropriateness of references, if applicable; and c.) format and completion of meeting clearance form if required

Comments: _____

Signature _____ Date _____

4. This request has been reviewed by PR for: a.) technical accuracy, b.) appropriateness for audience, c.) appropriateness of distribution statement, d.) technical sensitivity and economic sensitivity, e.) military/national critical technology, and f.) data rights and patentability

Comments: _____

APPROVED/APPROVED AS AMENDED/DISAPPROVED

PHILIP A. KESSEL Date
Technical Advisor
Propulsion Science and Advanced Concepts Division

In pursuit of the PO_2^+ cation. The reaction of KPO_2F_2 and SbF_5 leads to an eight-membered, antimony-oxygen-phosphorus-bridged ring[†]

Stefan Schneider^a, Ashwani Vij^b, Jeffrey A. Sheehy^b, Fook S. Tham^c, Thorsten Schroer^a, and Karl O. Christe^{a,b,*}

^aLoker Hydrocarbon Research Institute, University of Southern California, University Park, Los Angeles, California 90089-1661, USA,

^bAir Force Research Laboratory, Edwards Air Force Base, California 93524, USA, and

^cUniversity of California, Riverside, California 92521, USA

Professor Josef Goubeau in memoriam

Bei der Redaktion eingegangen am

Abstract. The reaction of KPO_2F_2 with the strong Lewis acid SbF_5 was studied as a potential pathway to the unknown PO_2^+ cation. The resulting product has the desired PO_2SbF_6 composition but consists of an eight-membered, oxygen-bridged ring that was

20021122 024

characterized by vibrational and NMR spectroscopy, *ab initio* methods, and a single crystal x-ray diffraction study. The formation of the oxygen-bridged ring and its mechanism are discussed.

Auf der Suche nach dem PO_2^+ Kation. Die Reaktion von KPO_2F_2 mit SbF_5 führt zu einem achtegliedrigen Sb-O-P verbrückten Ring

Inhaltsübersicht. Auf der Suche nach dem PO_2^+ Kation wurde die Reaktion von KPO_2F_2 mit der starken Lewisäure SbF_5 untersucht. Das resultierende Produkt mit der gewünschten Zusammensetzung PO_2SbF_6 besteht aus einem achtegliedrigen sauerstoffverbrückten Ring der anhand von schwingungs-, NMR-spektroskopischen und *ab initio* Methoden sowie einer Einkristallröntgenstrukturuntersuchung charakterisiert wurde. Der Mechanismus und die Bildung des sauerstoffverbrückten Rings werden diskutiert.

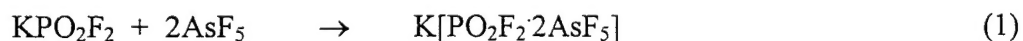
Keywords: Phosphoryl cation, eight-membered, P-O-Sb bridged ring, vibrational spectroscopy, NMR spectroscopy, crystal structure, *ab initio* calculations

* Corresponding author

Prof. Dr. Karl O. Christe
University of Southern California
Loker Hydrocarbon Research Institute
Los Angeles, CA 90089-1661, USA
e-mail: karl.christe@edwards.af.mil

Introduction

In view of the long known existence, great stability and general utility of CO_2 , SiO_2 and NO_2^+ , it is surprising that the closely related PO_2^+ cation is presently still unknown. The only data available is an *ab initio* calculation on the free gaseous ion [1]. Very little is also known about its parent molecule, phosphoryl fluoride [2,3], however, the corresponding anion, PO_2F_2^- , is well known and characterized [4]. Since anions can generally be converted to the corresponding parent molecules and cations by treatment with a strong Lewis acid, it was interesting to study the reaction of a PO_2F_2^- salt with strong Lewis acids. In a previous study in our laboratory, the interaction between KPO_2F_2 and AsF_5 had been studied [5]. Surprisingly, only an oxygen-bridged polynuclear anion between PO_2F_2^- and two AsF_5 molecules (eq. (1), Fig. 1) and no PO_2F or PO_2^+ were observed.



The failure to generate the PO_2^+ cation in this reaction can be attributed to PO_2F having a Lewis acidity comparable to that of AsF_5 [6, 7]. Therefore, PO_2F_2^- shares its oxygen ligands with AsF_5 through the formation of a donor-acceptor adduct rather than give up fluoride ions to form PO_2F or the PO_2^+ cation. Since SbF_5 and particularly oligomeric SbF_5 are much stronger Lewis acids than AsF_5 [6], it was hoped that the replacement of AsF_5 in reaction (1) by an excess of SbF_5 might lead to PO_2^+ .

Another highly interesting aspect is the most plausible structure of PO_2^+ . Whereas the minimum energy structure of the free gaseous PO_2^+ ion is a di-coordinated linear monomer [1] as in CO_2 and NO_2^+ , the condensed phase structure of PO_2^+ is more problematic. Since phosphorus seeks a coordination number higher than two, the PO_2^+ cations would either have to polymerize, as isoelectronic SiO_2 does, or undergo fluorine or oxygen bridging with the anions. Of these two choices, the first one is less likely because it would result in an accumulation of mutually repelling positive charges.

Experimental

Materials and Methods

All volatile materials were handled in either a stainless-steel vacuum line [8] equipped with Teflon-FEP U-traps, 316 stainless-steel bellows-seal valves, and a Heise Bourdon tube-type pressure gauge, or a flamed-out Pyrex glass vacuum line equipped with grease-free Kontes glass Teflon valves. Nonvolatile materials were handled in the dry nitrogen atmosphere of a glove box.

Infrared spectra were recorded in the range of $4000\text{--}400\text{ cm}^{-1}$ on a Midac FT-IR Model 1720 at a resolution of 1 cm^{-1} . Spectra of solids were obtained by using dry powders pressed between AgCl windows in an Econo press (Barnes Engineering Co.). Spectra of gases were obtained by using a stainless steel cell of 5 cm path length equipped with AgCl windows. Raman spectra were recorded in the range of $4000\text{--}10\text{ cm}^{-1}$ on a Bruker Equinox 55 FT-RA spectrophotometer using a NdYag laser at 1064

nm. Pyrex melting point capillaries or NMR tubes, that were baked out at 300 °C for 48 h at 10 mtorr vacuum, were used as sample containers.

The ^{19}F and ^{31}P NMR spectra were recorded on a Bruker AM-360 spectrometer equipped with a 8.45556-T cryomagnet. Samples were measured in heat sealed 4mm glass tubes and referenced to CFCl_3 (^{19}F) and 85% H_3PO_4 (^{31}P) at 20°C with positive shifts being to high frequency of the reference compounds.

Commercially available urea, KH_2PO_4 (Aldrich), NH_4HF_2 (Riedel-de-Haen) and SO_2 (Matheson) were used as received. SbF_5 (Ozark Mahoning) was purified by distillation prior to use. A literature method was used for the preparation of KPO_2F_2 [9] and it showed no impurities detectable by vibrational spectroscopy.

Single crystals of $(\text{SbF}_4\text{O}_2\text{PF}_2)_2$ were grown by slow sublimation at 90°C. They were mounted on the goniometer head by the oil-drop method using perfluoropolyether (PFPE) oil and precentered Nylon Cryoloops equipped with a magnetic base. The crystal structure was determined at 203 K using a Bruker diffractometer equipped with a CCD detector and a low temperature, LT3, device. The 3-circle platform with a fixed χ -axis was controlled by the SMART [10] software package. The unit cell parameters were determined from three runs of data with 30 frames per run using a scan speed of 30-seconds per frame. A complete hemisphere of data was collected using 1271 frames at 30 sec/frame, including 50 frames that were collected at the beginning and end of the data collection to monitor crystal decay. Data were integrated using the SAINT [11] software package, and the raw data was corrected for absorption using the SADABS [12] program. The structure was solved by the Patterson method using the SHELXS-97 [13] program and refined by the least squares method on F^2 using SHELXL-97 [14]. The crystal did not show any significant decomposition during the data collection. The

experimental and refinement parameters, and the atomic coordinates and thermal displacement parameters are listed in Tables 1 and 2, respectively.

Computational Methods

Infrared and Raman spectra for oxygen- and fluorine-bridged $(\text{SbF}_4\text{O}_2\text{PF}_2)_2$ complexes were computed by the density-functional approach using the B3LYP functional [15]. The so-called DFT/DZVP all-electron basis set [16,17], supplemented with one f function with an exponent of 0.3854 taken from the polarization functions of Ahlrichs [18], was used for antimony, and 6-311G(d) basis sets of Pople *et al.* [19] were used for oxygen, phosphorus, and fluorine. Cartesian coordinates taken from crystal structure determinations were used as a starting point for the geometry optimizations. The calculations were carried out on IBM RS/6000 Model 260 workstations using the Gaussian 98 [20] program system.

Syntheses of $(\text{SbF}_4\text{O}_2\text{PF}_2)_2$ and $\text{KPO}_2\text{F}_2 \cdot 2\text{SbF}_5$

In the drybox, KPO_2F_2 (6.39 mmol) was placed into a flamed-out Pyrex glass reaction vessel equipped with a grease-free Kontes glass Teflon valve. On the metal vacuum line, a large excess of SbF_5 (34.23 mmol) and a few ml of SO_2 were added to the reaction vessel. After keeping the mixture at room temperature for several hours, the SO_2 and unreacted SbF_5 were pumped off and pure, crystalline $(\text{SbF}_4\text{O}_2\text{PF}_2)_2$ was obtained in high yield by vacuum sublimation at 95 °C. The colorless solid residue consisted of KSbF_6 that was identified by vibrational spectroscopy and the observed mass balance.

In another experiment, a 1:2 mixture of KPO_2F_2 (13.52 mmol) and SbF_5 (27.2 mmol) was placed into a flamed-out Pyrex glass vessel. After a couple of weeks at room temperature, all the liquid SbF_5 had reacted with KPO_2F_2 resulting in a dry colorless powder. A comparison of the vibrational spectra of the product with those of the $\text{KPO}_2\text{F}_2 \cdot 2\text{AsF}_5$ polyanion [5] showed, that the product had the composition $\text{KPO}_2\text{F}_2 \cdot 2\text{SbF}_5$.

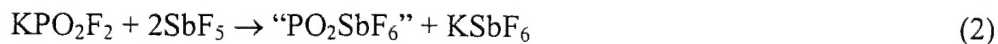
Raman spectral data for $\text{KPO}_2\text{F}_2 \cdot 2\text{SbF}_5$ (dry powder) [cm^{-1} (relative intensity)]: 232(12.8), 294(38.5), 598(2.6), 613(5.1), 659(100), 689(15.4), 956(7.7).

Heating of $\text{KPO}_2\text{F}_2 \cdot 2\text{SbF}_5$ to 95 °C resulted in the sublimation of $(\text{SbF}_4\text{O}_2\text{PF}_2)_2$. Further heating of $(\text{SbF}_4\text{O}_2\text{PF}_2)_2$ led to slow POF_3 evolution and produced a colorless liquid of undetermined composition.

Results and Discussion

Synthesis and Properties of $(\text{SbF}_4\text{O}_2\text{PF}_2)_2$

The room-temperature reaction of KPO_2F_2 with excess SbF_5 in the presence of a suitable solvent, such as SO_2 , followed by the removal of the solvent and excess SbF_5 and a vacuum sublimation at 95 °C, produces KSbF_6 and a product of the desired composition PO_2SbF_6 (eq. 2).



The more volatile "PO₂SbF₆" can be readily separated from the KSbF₆ by vacuum sublimation at 95 °C and was obtained in high yield and purity. As will be shown below, this compound does not have a simple PO₂⁺SbF₆⁻ structure but consists of eight-membered, oxygen-bridged (SbF₄O₂PF₂)₂ units.

A compound with such a structure has been proposed previously by *Krüger, Dehnicke, and Shihada* [21]. It was isolated in 4% yield from the reaction of SbF₅ with HOPOF₂ (eq. 3).



However, its reported properties (fine, white crystals, m.p. 65 °C, decomp.p. 70°C with POF₃ loss) do not agree well with those observed by us for (SbF₄O₂PF₂)₂ (crystalline solid, stable at 95 °C). Also the reported IR spectrum (1230 vs, 1175 s, 1095 w, 1042 s, 961 m, 735 s, 705 vs, etc) shows only fair agreement with our data (see below), but their ³¹P NMR spectrum agrees well with that observed in this study. Although in our opinion, *Krüger, Dehnicke and Shihada* had probably prepared the same compound and suggested, by analogy with related known compounds, the correct oxygen-bridged dimeric structure, their compound may have been of poor purity and was not well characterized.

Crystal structure of $(\text{SbF}_4\text{O}_2\text{PF}_2)_2$

The crystals of $(\text{SbF}_4\text{O}_2\text{PF}_2)_2$ belong to the centrosymmetric space group P-1. The asymmetric unit cell contains one half of the dimer and the other half is generated by the symmetry operation $-x+1, -y+2, -z$. The structure of $(\text{SbF}_4\text{O}_2\text{PF}_2)_2$ (Fig. 2, Table 3) shows that the molecule contains an eight-membered $[\text{Sb-O-P-O}]_2$ ring which adopts a chair conformation where two SbF_4 units are bridged by two $-\text{OP}(\text{F}_2)\text{O}-$ groups. The phosphorus and oxygen atoms are coplanar with a maximum mean plane deviation of 0.0186 Å and the antimony atoms are located above and below this plane at 1.1418 Å. There is a significant distortion of the octahedral environment around the antimony atoms due to the two bridging oxygen ligands having considerably longer bonds and, therefore, being less repulsive. The fluorine atoms F1 and F2 are located in a quasi-axial position and are longer by 0.02 Å (average $\text{Sb-F} = 1.865$ Å) compared to the equatorial fluorine atoms F3 and F4 (average $\text{Sb-F} = 1.845$ Å). The two Sb-O distances are practically identical at 2.004(4) Å and 2.003(4) Å. Due to the presence of the two longer Sb-O bonds, the F1-Sb1-F2 angle is compressed to $171.2(2)^\circ$ from the ideal value of 180° , the O-Sb-O angle is compressed to $86.4(2)$, and the F3-Sb1-F4 angle is widened to $93.6(2)^\circ$. A comparison of the bond distances and angles for $(\text{SbF}_4\text{O}_2\text{PF}_2)_2$ with those of closely related SbCl_4 derivatives [22, 23] is listed in Table 4 and shows good agreement.

The crystal packing diagram of $(\text{SbF}_4\text{O}_2\text{PF}_2)_2$ along the b -axis is shown in Fig. 3. The chair-form molecules make contacts with the neighboring molecules resulting in a polymeric chain. The closest contact distances are $\text{P1}\cdots\text{F2}$ and $\text{P1}\cdots\text{F3}$ at 3.295 and 3.277 Å, respectively.

Since oxygen and fluorine atoms are often difficult to distinguish in crystal structures, the possibility of refining our data set for a fluorine-bridged model was also explored. It resulted in a significantly higher R factor and larger thermal parameters of the bridging atoms and was therefore rejected. Further support for the oxygen-bridged model comes from the vibrational spectra and theoretical calculations.

Vibrational Spectra and Theoretical Calculations

The Raman and infrared spectra of $(\text{SbF}_4\text{O}_2\text{PF}_2)_2$ are shown in Fig. 4. The observed and calculated vibrational frequencies and IR and Raman intensities are summarized in Table 5. For comparison, the calculated spectra of the fluorine-bridged model have also been listed in this table. As can be seen from Table 5, the observed spectra agree only with the oxygen-bridged but not with the fluorine-bridged model. In a fluorine-bridged structure, the P-O bonds would possess significant double bond character and their antisymmetric stretching vibrations should occur in the 1500 cm^{-1} region.

The assignments for $(\text{SbF}_4\text{O}_2\text{PF}_2)_2$ were made in point group C_i , in accord with the results from the crystal structure determination and the theoretical calculations which show that $(\text{SbF}_4\text{O}_2\text{PF}_2)_2$ possesses only a symmetry center and that no atoms lie on this center. A total of 54 fundamental vibrations are expected out of which one half of them is symmetric (A_g modes) and the other half is antisymmetric (A_u modes) to the symmetry center. The A_g modes are due to the in-phase motions of the symmetry related groups and are only Raman active, while the A_u modes represent the out-of-phase motions of these groups and are only infrared active. Since the vibrational coupling

between the corresponding A_g and A_u modes is relatively weak, their frequency separations are small, except for the four highest frequency modes that are due to the antisymmetric and symmetric in-phase and out-of-phase stretching motions of the PO_2 groups. Therefore, it may appear that some of the bands are active in both the infrared and the Raman spectra, but a closer inspection reveals that their frequencies differ enough to rule out this interpretation. In view of the complexity of the symmetry coordinates for such a large system, a normal coordinate analysis was not carried out for $(SbF_4O_2PF_2)_2$.

The total energies, calculated for the oxygen- and the fluorine-bridged structures show that the oxygen-bridged model is favored by $130 \text{ kcal mol}^{-1}$. This large energy difference accounts for the preferred formation of the oxygen-bridged rings which can be explained by the following mechanism (Fig. 5).

The first step involves the formation of an oxygen-bridged polynuclear $[PO_2F_2 \cdot 2SbF_5]^-$ anion, as in the case of AsF_5 . The important difference between AsF_5 and SbF_5 is that antimony can expand its coordination towards fluorine or oxygen past six, while arsenic cannot [24]. This allows the SbF_5 ligand of $[PO_2F_2 \cdot 2SbF_5]^-$ to interact with a second $PO_2F_2^-$ anion, as shown in Figure 5. Elimination of two equivalents of KF then produces the final product. The following experimental evidence supports this mechanism. When a 2:1 molar mixture of SbF_5 and KPO_2F_2 was allowed to interact at room temperature in the absence of a solvent, a colorless powder was obtained that was identified by vibrational spectroscopy as the K^+ salt of the oxygen bridged $[PO_2F_2 \cdot 2SbF_5]^-$ polyanion. Heating of this salt to $95^\circ C$ resulted in the sublimation of $(SbF_4O_2PF_2)_2$ and a $KSbF_6$ residue (see Experimental Section).

NMR Spectra

A solution of a few single crystals of $(\text{SbF}_4\text{O}_2\text{PF}_2)_2$ in SO_2 was used to record NMR-spectra. The strongest signal in the ^{31}P spectra was a triplet (δ -35.6 ppm, $^1J_{\text{PF}}$ 1030 Hz) that is typical for a PO_2F_2 group, but the spectra also exhibited many signals that could not be firmly assigned. The chemical shift and the $^1J_{\text{PF}}$ coupling constant observed for our triplet agree well with those (t, δ -35.5 ppm, $^1J_{\text{PF}}$ 1039 Hz) previously reported by *Dehnicke* et al [21] for an SbF_5 solution. The ^{19}F NMR-spectra were even more complicated. Only the signal for the PO_2F_2 -group (d, δ -80.5 ppm, $^1J_{\text{PF}}$ 1037 Hz) could be assigned. In view of this, it is not certain whether the eight-membered ring persists in SO_2 solution at room temperature.

Conclusion

The reaction of KPO_2F_2 with the strongest presently known Lewis acid, i.e., oligomeric SbF_5 , does not produce PO_2^+ salts but oxygen-bridged eight-membered Sb-O-P rings with hexa-coordinated antimony and tetra-coordinated phosphorus. The chances for preparing ionic salts that contain isolated PO_2^+ cations must be considered very slim because pentavalent phosphorus seeks coordination numbers in excess of two. Since the polymerization of PO_2^+ is highly unlikely due to the mutual repulsion of charges of the same sign, PO_2^+ exhibits a strong tendency to undergo oxygen- or fluorine- bridging to

achieve higher coordination. Even the possibility of approximating a PO_2^+ cation by having a PO_2F_2^- unit forming two fluorine-bridges to very strong Lewis acids is thwarted by energetics. In the eight-membered $(\text{SbF}_4\text{O}_2\text{PF}_2)_2$ rings, the oxygen-bridged structure is favored over the fluorine-bridged one by $130 \text{ kcal mol}^{-1}$.

Acknowledgement

The work at USC was financially supported by the National Science Foundation and that at the Air Force Research Laboratory by the Air Force Office of Scientific Research and DARPA. Two of us (S.S. and T.S.) gratefully acknowledge support by the Alexander von Humboldt Foundation.

References

- [1] P. Pyykkö, Y. Zhao, *Mol. Phys.* **1990**, *70*, 701.
- [2] U. Wannagat, J. Rademachers, *Z. Anorg. Allg. Chem.* **1957**, 289, 66.
- [3] D. W. Muenow, O. M. Uy, J. L. Margrave, *J. Inorg. Nucl. Chem.* **1969**, *31*, 3411.
- [4] A. Addou, P. Vast, P. Legrand, *Spectrochim. Acta, Part A* **1982**, *38A*, 785, and references cited therein.
- [5] K. O. Christe, R. Gnann, R. I. Wagner, W. W. Wilson, *Eur. J. Solid State Inorg Chem.* **1996**, *33*, 865.
- [6] J. W. Larson, T.B. McMahon, *Inorg. Chem.* **1987**, *26*, 4018.

- [7] K. O. Christe, D. A. Dixon, D. McLemore, W.W. Wilson, J. A. Sheehy, J. A. Boatz, *J. Fluorine Chem.* **2000**, *101*, 151.
- [8] K. O. Christe, R. D. Wilson, C. J. Schack, *Inorg. Synth.* **1986**, *24*, 3.
- [9] U. Schuelke, R. Kayser, *Z. Anorg. Allg. Chem.* **1991**, *600*, 221.
- [10] SMART V 4.045 Software for the CCD Detector System, Bruker AXS, Madison, WI 1999.
- [11] SAINT V 4.035 Software for the CCD Detector System, Bruker AXS, Madison, WI 1999.
- [12] SADABS, Program for absorption correction for area detectors, Version 2.01, Bruker AXS, Madison, WI 2000.
- [13] G. M. Sheldrick, SHELXS-97, Program for the Solution of Crystal Structure, University of Göttingen, Germany, 1997.
- [14] G. M. Sheldrick, SHELXL-97, Program for the Refinement of Crystal Structure, University of Göttingen, Germany, 1997.
- [15] The B3LYP functional uses a three-parameter exchange functional of Becke (B3) [A.D. Becke, *J. Chem. Phys.* **1993**, *98*, 5648; P.J. Stephens, C.F. Devlin, C.F. Chabalowski, and M.J. Frisch, *J. Phys. Chem.* **1994**, *98*, 11623] and the Lee, Yang, and Parr (LYP) correlation gradient-corrected functional [C. Lee, W. Yang, and R.G. Parr, *Phys. Rev. B* **1988**, *37*, 785].
- [16] These local-spin-density-optimized Gaussian basis sets were developed by Nathalie Godbout and Jan Andzelm, and are made available courtesy of Cray Research, Inc. The general method by which they were developed is given in N.

- Godbout, D.R. Salahub, J. Andzelm, and E. Wimmer, *Can. J. Chem.* **1992**, *70*, 560.
- [17] Basis sets were obtained from the Extensible Computational Chemistry Environment Basis Set Database, Version , as developed and distributed by the Molecular Science Computing Facility, Environmental and Molecular Sciences Laboratory which is part of the Pacific Northwest Laboratory, P.O. Box 999, Richland, Washington 99352, USA, and funded by the U.S. Department of Energy. The Pacific Northwest Laboratory is a multi-program laboratory operated by Battelle Memorial Institute for the U.S. Department of Energy under contract DE-AC06-76RLO 1830. Contact David Feller or Karen Schuchardt for further.
- [18] Polarization functions are unpublished supplements to the basis sets described in A. Schafer, C. Huber, and R. Ahlrichs, *J. Chem. Phys.* **1994**, *100*, 5829.
- [19] M.J. Frisch, J.A. Pople, and J.S. Binkley, *J. Chem. Phys.* **1984**, *80*, 3265.
- [20] Gaussian 98, Revision A.7, M.J. Frisch, G.W. Trucks, H.B. Schlegel, G.E. Scuseria, M.A. Robb, J.R. Cheeseman, V.G. Zakrzewski, J.A. Montgomery, R.E. Stratmann, J.C. Burant, S. Dapprich, J.M. Millam, A.D. Daniels, K.N. Kudin, M.C. Strain, O. Farkas, J. Tomasi, V. Barone, M. Cossi, R. Cammi, B. Mennucci, C. Pomelli, C. Adamo, S. Clifford, J. Ochterski, G.A. Petersson, P.Y. Ayala, Q. Cui, K. Morokuma, D.K. Malick, A.D. Rabuck, K. Raghavachari, J.B. Foresman, J. Cioslowski, J.V. Ortiz, B.B. Stefanov, G. Liu, A. Liashenko, P. Piskorz, I. Komaromi, R. Gomperts, R.L. Martin, D.J. Fox, T. Keith, M.A. Al-

- Laham, C.Y. Peng, A. Nanayakkara, C. Gonzalez, M. Challacombe, P.M.W. Gill, B.G. Johnson, W. Chen, M.W. Wong, J.L. Andres, M. Head-Gordon, E.S. Replogle, and J.A. Pople, Gaussian, Inc., Pittsburgh, PA, 1998.
- [21] N. Krüger, K. Dehnicke, A. F. Shihada, *Z. Anorg. Allg. Chem.* **1978**, 438, 169.
- [22] A. W. Cooke, J. Pebler, F. Weller, K. Dehnicke, *Z. Anorg. Allg. Chem.* **1985**, 524, 68.
- [23] A. F. Shihada, F. Weller, *Z. Anorg. Allg. Chem.* **1981**, 472, 102.
- [24] G. W. Drake, D. A. Dixon, J. A. Sheehy, J. A. Boatz, K. O. Christe, *J. Am. Chem. Soc.* **1998**, 120, 8392.

Table 1. Crystal data and structure refinement for (SbF₄O₂PF₂)₂.

Empirical formula	F ₁₂ O ₄ P ₂ Sb ₂
Space group	P-1 triclinic
Unit cell dimensions	a = 5.565(4) Å α = 88.685(16)°. b = 7.406(6) Å β = 76.367(16)°. c = 7.443(6) Å γ = 83.364(16)°.
Volume / Å ³	296.1(4)
ρ _(calculated) / g cm ⁻³	3.350
Z	2
Formula weight	597.44
μ / mm ⁻¹	5.001
Temperature / K	203(2)
λ (MoKα) / Å	0.71073
Crystal size / mm	0.20 x 0.12 x 0.10
Theta range for data collection θ / °	2.77 to 26.37
Index ranges (hkl)	-6 ≤ h ≤ 6, -9 ≤ k ≤ 9, -9 ≤ l ≤ 9
Reflections collected	2845
Independent reflections	1202 [R(int) = 0.0469]
F(000)	272
Max. and min. transmission	0.565765 and 0.406416
R ^a [I > 2σ(I)]	R1 = 0.0406, wR2 = 0.0987
R ^a (all data)	R1 = 0.0416, wR2 = 0.0997
Largest diff. peak and hole (e Å ⁻³)	2.174 and -1.864
Absorption correction	SADABS
Goodness-of-fit on F ²	1.168
Data / restraints / parameters	1202 / 0 / 91
Refinement method	Full-matrix least-squares on F ²

(a) $R = \sum |F_o| - |F_c| / \sum |F_o|$.

Table 2. Atomic coordinates ($\times 10^4$) and equivalent isotropic displacement parameters ($\text{\AA}^2 \times 10^3$).

	X	Y	z	U(eq) ^a
Sb(1)	4170(1)	7691(1)	2440(1)	20(1)
P(1)	2277(2)	11935(2)	1685(2)	20(1)
F(1)	6657(6)	9178(5)	2470(6)	32(1)
F(2)	1648(6)	6397(5)	2075(5)	29(1)
F(3)	2636(8)	8157(6)	4885(5)	38(1)
F(4)	6091(8)	5603(5)	2912(6)	39(1)
O(2)	4353(8)	12637(6)	276(6)	28(1)
O(1)	2190(7)	9927(5)	1761(6)	26(1)
F(6)	-202(6)	12778(5)	1420(5)	33(1)
F(5)	2419(7)	12638(5)	3522(5)	33(1)

$$U_{eq} = (1/3) \sum_i \sum_j U_{ij} \mathbf{a}_i^* \mathbf{a}_j^* \mathbf{a}_i \mathbf{a}_j$$

Table 3. Bond lengths [\AA] and selected angles [$^\circ$] for $(\text{SbF}_4\text{O}_2\text{PF}_2)_2$ ^[a].

Sb(1)-F(3)	1.841(4)	F(3)-Sb(1)-F(2)	93.0(2)
Sb(1)-F(4)	1.851(4)	F(2)-Sb(1)-F(1)	171.1(2)
Sb(1)-F(2)	1.861(3)	F(2)-Sb(1)-O(2)#1	86.3(2)
Sb(1)-F(1)	1.870(4)	F(4)-Sb(1)-O(1)	176.4(2)
Sb(1)-O(2)#1	2.003(4)	O(2)#1-Sb(1)-O(1)	86.4(2)
Sb(1)-O(1)	2.004(4)	O(1)-P(1)-F(5)	110.4(2)
P(1)-O(1)	1.493(4)	O(1)-P(1)-O(2)	117.3(2)
P(1)-F(5)	1.497(4)	F(5)-P(1)-O(2)	106.6(2)
P(1)-O(2)	1.499(4)	O(1)-P(1)-F(6)	106.8(2)
P(1)-F(6)	1.502(3)	F(5)-P(1)-F(6)	104.5(2)
		O(2)-P(1)-F(6)	110.6(2)
		P(1)-O(2)-Sb(1)#1	136.8(3)
		P(1)-O(1)-Sb(1)	138.7(3)

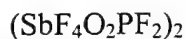
Symmetry transformations used to generate equivalent atoms: #1 -x+1,-y+2,-z

[a] further details about the investigation of the crystal structure can be requested from: Fachinformationszentrum Karlsruhe, D-76344 Eggenstein-Leopoldshafen, Germany, E-mail crysdata@fiz-Karlsruhe.de, under number CSD-XXXXXX.

Table 4. Comparative bond distances [\AA] and angles [$^\circ$] (in $(\text{SbF}_4\text{O}_2\text{PF}_2)_2$, $(\text{SbCl}_4\text{O}_2\text{PCl}_2)_2$ and $(\text{SbCl}_4\text{O}_2\text{PMe}_2)_2$

	$(\text{SbF}_4\text{O}_2\text{PF}_2)_2^{[a]}$	$(\text{SbCl}_4\text{O}_2\text{PCl}_2)_2^{[22]}$	$(\text{SbCl}_4\text{O}_2\text{PMe}_2)_2^{[23]}$
Sb-O (av)	2.004(4)	2.06	2.01
Sb-X (X = F or Cl) (av)	1.856(4)	2.30	2.35
P-O (av)	1.496(4)	1.50	1.55
O-Sb-O	86.4(2)	83	87
O-P-O	117.3(2)	116	113

[a] present work



Calcd frequencies [cm^{-1}] ^[a]		Obsd frequencies [cm^{-1}] ^[b]		Calcd frequencies [cm^{-1}] ^[a]		Assignment in point Group C_i	
B3LYP Oxygen-bridged				B3LYP Fluorine-bridged			
Raman	IR	Raman	IR	Raman	IR		
	1252 (1297)		1261 (vs)	1507	1509 (289)	v 28	(Au)
1167 [10]dp		1161 [3]		1147		v 1	(Ag)
1158 [4]p						v 2	(Ag)
	1137 (989)		1158 (vs)		1144 (157)	v 29	(Au)
	991 (409)		1046 (s)		744 (174)	v 30	(Au)
985 [4]dp		1048 [7]		742		v 3	(Ag)
907 [16]p		960 [19]			717 (178)	v 4	(Ag)
	899 (72)		952 (s)	715		v 31	(Au)
	724 (181)		708 (vs,br)	705		v 32	(Au)
721 [3]p		710 [5]			702 (124)	v 5	(Ag)
695 [3]dp		509 [2]			652 (16)	v 6	(Ag)
	693 (156)		684 (vs)	651		v 33	(Au)
687 [12]p		691 [39]		506		v 7	(Ag)
	685 (203)		637 (m)		472 (94)	v 34	(Au)
620 [21]p		632 [100]		467		v 8	(Ag)
	619 (1)				463 (881)	v 35	(Au)
	590 (63)			461		v 36	(Au)
582 [0.2]p					454 (0.3)	v 9	(Ag)
491 [2]p			488 (s)		432 (630)	v 10	(Ag)
	481 (95)				403 (27)	v 37	(Au)
470 [2]p			458 (sh)	400		v 11	(Ag)
	464 (134)			356		v 38	(Au)
440 [12]p		461 [11]			347 (9)	v 12	(Ag)
	433 (13)			330		v 39	(Au)
358 [0.4]p		382 [1]		298		v 13	(Ag)
	345 (45)				281 (120)	v 40	(Au)
276 [1]p		270 [26]		253		v 14	(Ag)
	271 (261)				252 (97)	v 41	(Au)
	269 (114)				248 (102)	v 42	(Au)
	258 (44)			246		v 43	(Au)
257 [2]p		253 [1]			245 (267)	v 15	(Ag)
	252 (10)			229		v 44	(Au)
246 [3]dp		240 [2]			222 (5)	v 16	(Ag)
243 [0.5]dp					215 (4)	v 17	(Ag)
	237 (5)				208 (10)	v 45	(Au)
	229 (0.3)			204		v 46	(Au)
217 [3]p		218 [4]		186		v 18	(Ag)
	209 (0.1)				180 (0.3)	v 47	(Au)
207 [1]dp				172		v 19	(Ag)
197 [2]p		196 [2]			166 (19)	v 20	(Ag)
	191 (4)			153		v 48	(Au)
177 [1]p				139		v 21	(Ag)
170 [0.02]p				121		v 22	(Ag)
	146 (1)				118 (0.04)	v 49	(Au)
	142 (0.1)				114 (2)	v 50	(Au)
133 [0.1]dp		151 [2]		111		v 23	(Ag)
108 [1]dp		118 [2]				v 24	(Ag)
	101 (0.01)					v 51	(Au)
52 [0.1]p						v 25	(Ag)
	48 (0.8)					v 52	(Au)
48 [0.02]p						v 26	(Ag)
	46 (0.9)					v 53	(Au)
32 [0.001]p						v 27	(Ag)
	21 (0.7)					v 54	(Au)

[a] IR intensities given in parentheses [km mol^{-1}], and Raman intensities given in brackets [$\text{A}^4 \text{amu}^{-1}$].

[b] Relative IR and Raman intensities given in parentheses and brackets, respectively.

Figure legends

Figure 1. Polynuclear anion $[\text{PO}_2\text{F}_2 \cdot 2\text{AsF}_5]^-$.

Figure 2. Ortep Plot of $(\text{SbF}_4\text{O}_2\text{PF}_2)_2$; thermal ellipsoids are shown at the 30% probability level.

Figure 3. Packing diagram of $(\text{SbF}_4\text{O}_2\text{PF}_2)_2$ along the *b*-axis showing the formation of a layered chain polymer through $\text{P} \cdots \text{F}$ bridges.

Figure 4. IR and Raman spectra of $(\text{SbF}_4\text{O}_2\text{PF}_2)_2$.

Figure 5. Formation mechanism of $(\text{SbF}_4\text{O}_2\text{PF}_2)_2$.

Figure 1

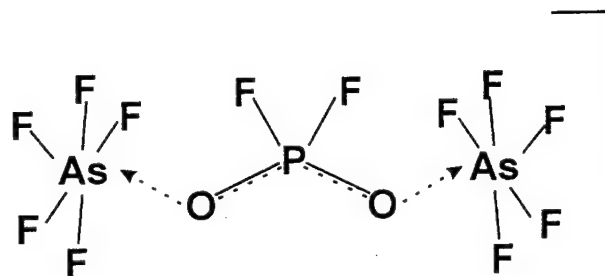


Figure 2

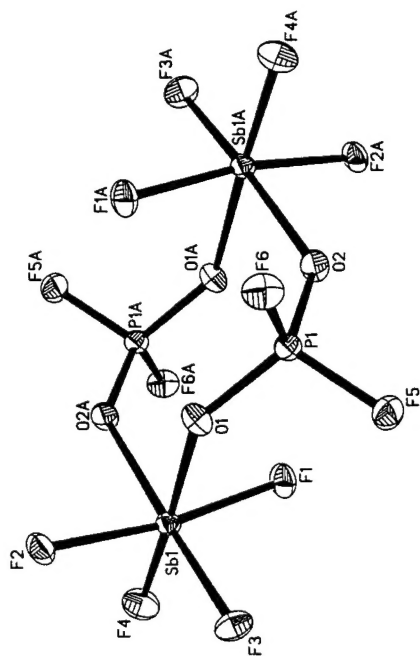


Figure 3

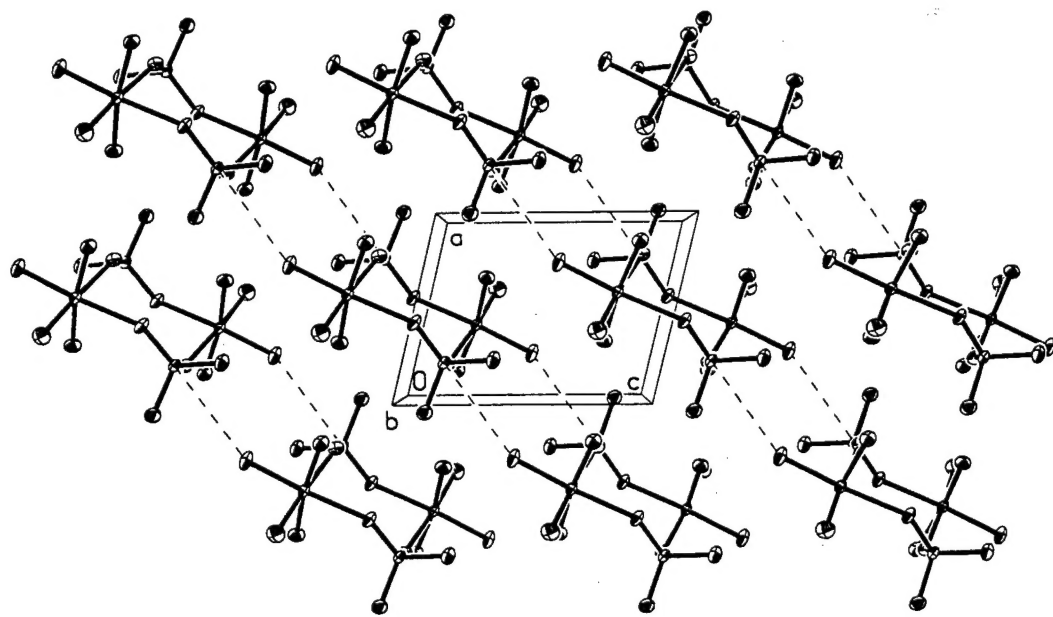


Figure 4

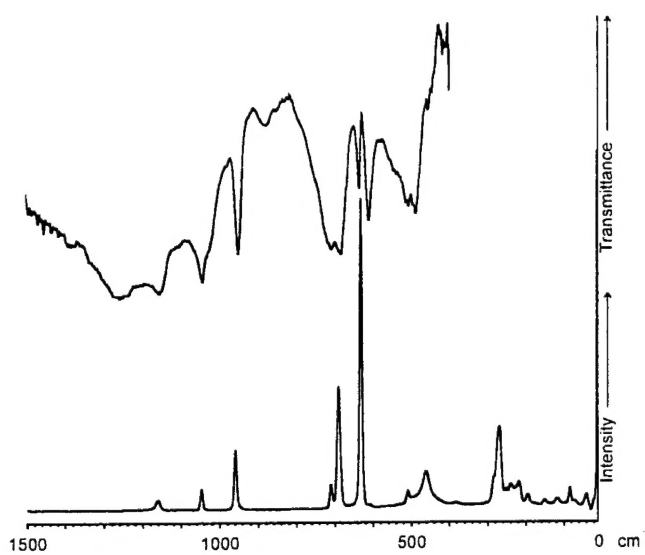


Figure 5

